A novel concept of passive knee prosthesis with multiple stiffnesses to support overground walking and sit-to-stand

Julien Guiaux Brinon[1] and Renaud Ronsse[1]

***Abstract*— Over the last decades, active knee prostheses demonstrated their ability to support most daily-life locomotion tasks for transfemoral amputees. However, passive devices are still used by a majority of patients due to their simplicity of use, low cost, independence with respect to an external power source, and adaptability across various gait profiles in daily tasks. A key challenge in the development of passive prostheses is to have them supporting the largest possible amount of locomotion tasks in a strictly passive manner. Following a recent trend promoting layered prostheses with active as-needed assistance, this paper focuses on the development of a passive knee prosthesis enabling walking on level ground and providing passive assistance for sit-to-stand-to-sit transitions. The fundamental feature on our innovative concept consists in relying on four passive mechanisms in order to render multiple stiffnesses adapted to the selected task or its specific phases (stance/swing). This paper reports the conceptual design of the prosthesis, its mechanical dimensioning, and a first embodiment fitting into the volume of existing devices.**

I. Introduction

Lower-limb amputation is a disabling condition affecting individual mobility, psychological health, and quality of life. Nowadays in Europe, about 20 per 100,000 inhabitants undergo a lower-limb amputation every year, with variations across ages, genders, and countries [1]. The predominant type of lower-limb amputation is transfemoral (i.e. above the knee), representing 55% of the total [2]. Moreover, the ongoing military conflicts in different places of the world are contributing to a significant surge in above-knee amputations [3]. Consequently, there is a growing demand for affordable and efficient prosthetic knee devices.

In recent years, research has focused on developing active knee prostheses to provide better functionality and adaptability for daily-life locomotion activities such as walking, climbing stairs, or standing up and sitting down. To date, several research prototypes emerged to address this challenge, such as the MIT Clutched Series Elastic Actuator (CSEA) [4], the CYBERLEGsPlusPlus [5], or the Utah Bionic Leg [6], among others. Moreover, two of such active systems are already commercially available, i.e. the Power Knee (Össur, Iceland) [7] and the INTUY Knee (Reboocon bionics, Netherlands) [8].

Even though these prostheses emulate sound leg dynamics during the majority of everyday locomotion tasks, the current standard-of-care in artificial knees is to use energetically passive devices [9, 10]. This is because the selection of a particular prosthesis is primarily dependent on the patient's level of autonomy in executing daily tasks. Only a minority of amputees — i.e. children, active adults, or athletes — require a prescription for an active prosthesis [11]. Moreover, passive devices are generally less expensive, simpler to use and manufacture, and are not affected by electronic reliability. For these reasons, they are still preferred by users or prescribed in developing regions and countries, especially if the demand rises for instance because of war.

Several research projects have focused on emulating the knee biomechanics with passive elements only. Some of them rely on a passive locking of the joint, thus missing capturing the compliant behavior of the knee during the weight acceptance phase and its associated benefits regarding shock absorption, balance support, and forward speed conservation [12, 13]. To remedy this, other projects then developed mechanisms to implement early stance knee flexion (ESF) relying on high stiffness elastic elements [11, 14] and/or on lower stiffness to render the swing phase behavior [5]. Similarly, one knee orthosis implemented a high-to-low-stiffness switch to approximate the behavior of both stance and swing [15]. Importantly, in all of these designs, transitioning between the high and low stiffnesses is done by an active module.

In parallel, a recent trend in research is promoting the use of passive components in active prostheses. This is motivated by a layered approach to lower-limb prostheses, aiming at performing the largest possible amount of tasks or phases of locomotion tasks in a strictly passive manner, and to add an "active as-needed assistance" for those tasks or phases only if strictly necessary [16, 17]. In parallel, several research groups are conducting the development of prostheses using mechanisms to passively carry out tasks that usually require the injection of energy, such as stairs ascent [18]. This is achieved by either energy exchanges between prosthetic knee and ankle modules or energy storage within the knee with delayed release [19].

In this paper, we adopt a similar strategy centered on cost-effectiveness and simplicity in prosthetic design, yet using only passive mechanisms in order to offer optimal functionality for daily mobility. In particular, we report an innovative concept for a passive knee prosthesis. The objective of this prosthetic device is to enable amputees to walk on level ground while capturing the biomechanics of natural gait as faithfully as possible. Additionally, it seeks to enhance motion transition capabilities by providing passive assistance while standing up and sitting down.

*This work was supported by the French Community of Belgium as part of FRIA grant (1.E014.24F awarded to JGB) from the F.R.S - FNRS.

[1]Julien Guiaux Brinon and Renaud Ronsse are with the Institute of Mechanics, Materials, and Civil Engineering; Louvain Bionics; and the Institute of Neuroscience; UCLouvain, Belgium julien.guiaux@uclouvain.be

The problem statement and prosthesis design guidelines are outlined in Section II. Section III describes the design of the mechanisms embodied in our prosthesis to emulate the above-mentioned tasks. The dimensioning of key functional components is discussed in Section IV. Finally, Section V concludes the paper and provides directions for future work.

II. Walking and sit-to-stand features and resulting design guidelines

An examination of the human knee angle-torque profile in both overground walking and transitions between standing and sitting is provided to motivate our device development.

A. Overground walking and stand-to-sit transition

Among daily locomotion tasks, walking on level ground is predominant. During normal walking, the human knee is required to produce significant extension and flexion torque in the sagittal plane (peaking at 56 Nm for an 80 kg individual). As depicted on a typical angle-torque profile (Fig. 1, solid blue line), the walking gait can be decomposed into two distinct phases corresponding to the stance and swing phases respectively. Stance is characterized by a small angular displacement (0 - 20°) with a linearly growing extension torque. This so-called weight acceptance allows absorbing the impact of the heel striking the ground. This decreases the joint stresses during impact and helps in stabilizing the body and conserving forward speed. Therefore, the knee can be well approximated by a stiff linear spring during this gait phase (Fig. 1, dashed orange-green line). In contrast, the swing phase is dominated by a higher angular motion (0 - 70°) with a lower torque profile. As a first approximation, this can be captured by a softer linear spring (Fig. 1, green solid line). Although this is a rough approximation, it is still acceptable, since following a precise position or torque profile is not essential for this phase. The key is to provide sufficient ground clearance when bending the knee and to reach the expected angle at next heel strike.

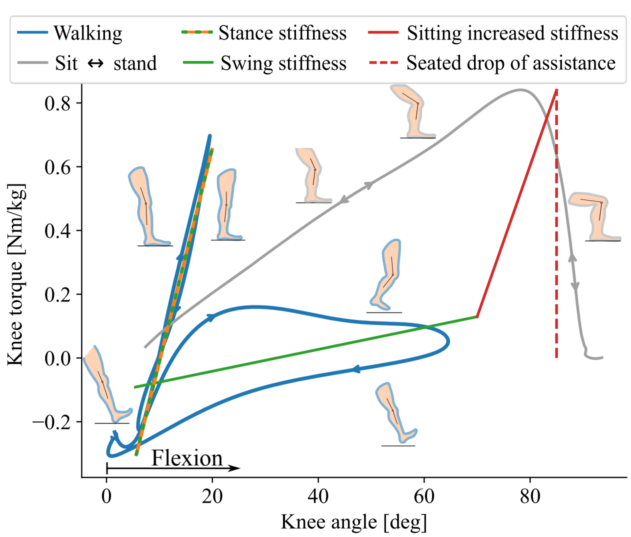

Fig. 1. Typical walking (blue) and sit-to-stand-to-sit (grey) knee angle-torque profile (derived from [20]). The other lines correspond to pure-spring behaviors approximating these curves during the stance phase of walking (dashed orange-green), the swing phase of walking (green), and the late sitting transition (red).

The second task considered in this paper is the transition between standing and sitting. From standing to sitting, as the knee undergoes flexion, it is imperative to supply a progressively rising extension torque to sustain the body weight and decelerate its descent. As depicted in Fig. 1 (grey solid line), the extension torque subsequently rapidly decreases upon sitting (at an angular position of about 75°), reaching zero to prevent a sudden re-extension of the leg once the body weight is transferred to the sitting support. The sit-to-stand transition follows a reverse trajectory.

B. Design guidelines

One way to passively reproduce the knee behavior for both considered tasks is to embed elastic elements in parallel to the joint, whose activation states vary as a function of the task and/or its phases. Focusing on walking first, our system should thus render a dual stiffness. It would have to provide high linear stiffness at the beginning of the stance phase (weight acceptance). Then, the device should render a lower joint stiffness for the late stance and swing phase. This is pictured in Fig. 2: first the parallel action of the swing spring (green) and the additional stance spring (orange) implements the stance stiffness (Fig. 1, dashed orange-green line). Then, only the lower swing stiffness (green) remains. A passive mechanism should trigger transitions between these two states by hiding the stiffer spring (orange) between the weight acceptance and late swing phases. This process should additionally occur smoothly and be robust over time.

The second design guideline is dictated by the stand-to-sit task. In active prosthesis, this shift in posture typically involves the assistance of an actuator in parallel to the joint. Yet, to accomplish this passively, it is necessary to develop a system impeding the descent with a torque that opposes flexion, in the same way the actuator would do in an active device. Our design hypothesis is that this behavior can be sufficiently well replicated by promptly augmenting the swing phase stiffness (Fig. 1, green solid line) once a

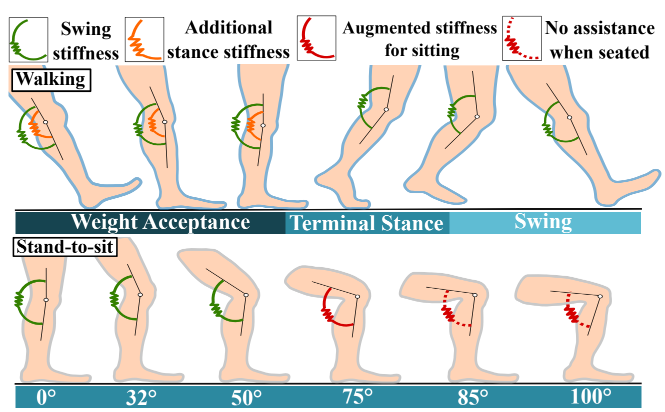

Fig. 2. Parallel stiffness states for walking (top) and stand-to-sit (bottom). For walking, the additional stance (orange) and swing (green) stiffnesses are placed in parallel with the knee joint. The additional stance spring is removed after weight acceptance. For stand-to-sit, the equivalent joint stiffness should further increase after a first angular threshold, and get hidden once seated.

predetermined angular threshold is exceeded (Fig. 1, red solid line). As illustrated in Fig. 2, this requires using a third elastic element or a mechanism with adjustable parallel linear stiffness that would be triggered at a given flexion angle (75° in Fig. 2).

Finally, next to this transition, it is required to cancel the extension torque once seated to avoid the leg from re-extending (Fig. 1, red dashed line). This high parallel stiffness should thus get hidden when a second angular threshold of 85° is reached, as shown in Fig. 2. Nevertheless, it is crucial to preserve the energy stored in the elastic elements to assist the user during the upcoming sit-to-stand transition. The compressed spring element should thus store its energy when seated while being hidden from the kinematic chain (Fig. 2, dashed red spring). An over-flexion (100° in Fig. 2) of the knee when seated would then be required to release the energy for assisting sit-to-stand.

C. Quantified specifications

The requirements for the prosthesis sub-mechanisms implementing the pre-cited guidelines can be derived assuming a typical user of 80 kg. Concerning the weight acceptance phase, the angular motion should range from 0° to 20° with a stiffness k_{st} of 290 Nm/rad. The rest position of the parallel spring must be around full extension (0°) and the high stiffness spring should allow reaching extension torques up to 56 Nm.

The swing stiffness implementation requires a range of motion between 0° and 75° with a lower stiffness k_{sw} of about 16 Nm/rad. A rest position corresponding to zero torque along the swing stiffness line should be defined and a peak torque of about 9 Nm in flexion must be achievable. Concerning the maximum extension torque in swing, the system must peak at 10 Nm before switching to a higher sitting stiffness k_{sit} of about 220 Nm/rad from an angular threshold of 75°. This stiffness should support stand-to-sit transition up to 85° leading to extension torque up to 67 Nm.

When seated, backward motion should be prevented after reaching this 85° threshold with the possibility to unlock the previously stored energy following an over-flexion of 100°. In this case, the assistive stored extension torque profile would follow the reverse trajectory, starting at 67 Nm and decreasing first abruptly, then smoothly.

III. Mechanical Design of the Prosthesis

This section reports the design of a passive prosthetic knee implementing the previously identified design guidelines. Fig. 3 shows an overview of the prosthesis and some of its key components. The device is symmetrical along its median sagittal plane. The knee joint consists of two pulleys (f) of radius r_p (depicted in Fig. 4, step 5) rotating around a main shaft. Two cables (i) transmit the efforts from various deformable elastic elements included in some sub-mechanisms to render the different joint stiffnesses identified in Section II-C.

At an angle corresponding to maximum extension, the prosthesis can transition between two configurations upon knee flexion. The first leads to the weight acceptance phase with the activation of a couple of high-stiffness elastically deformable elements implemented by composite beams working in flexion (k). The second disengages these beams and results in a lower stiffness for the swing phase and sitting task. The mechanisms allowing these transitions and their detailed operations are described hereafter.

A. Clutch for stance stiffness engagement

The stance mechanism should engage the high stiffness behavior during the weight acceptance phase. On the first hand, it consists of two elastically deformable elements implemented by composite beams working in flexion (Fig. 3, k). On the other hand, a system couples these beams with

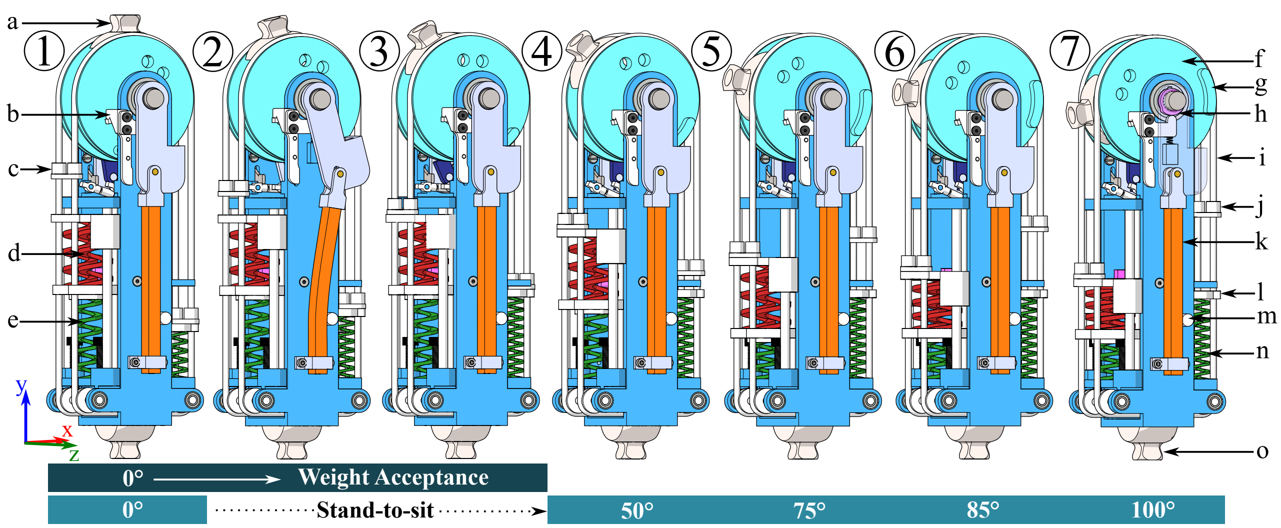

Fig. 3. Overview of the prosthesis during the walking weight acceptance phase (steps 1-3) and stand-to-sit transition (steps 1 and 4-7). The device components are: (a) upper connection pyramid, (b) reset mechanism, (c) double stiffness cable stopper, (d) sitting stiffness spring (two springs, each of stiffness k_1), (e) swing stiffness spring (extension torque, one spring of stiffness k_2), (f) main pulley, (g) pulley side appendage (stance stiffness mechanism), (h) stance reset cam, (i) transmission cable, (j) swing stiffness cable stopper, (k) stance stiffness deformable beam (Young modulus E), (l) swing stiffness mechanism carriage, (m) stance stiffness adjustment fulcrum, (n) swing stiffness spring (flexion torque, two springs), and (o) lower connection pyramid.

the knee joint through both main pulleys (Fig. 3, f). This system further implements the locking and unlocking at full extension angle. The stiffness and maximum torques can be adjusted by displacing the intermediate fulcrum constraining the beam displacement (Fig. 3, m).

The composite beams implement together an additional stance stiffness k_b. Therefore, their combined parallel effect with the swing stiffness k_{sw} renders the stance stiffness $k_{st} = k_{sw} + k_b$. These beams are characterized by a rectangular cross-section of depth h (Fig. 5, left) and width w. The loading configuration observable in Fig. 5 corresponds to an overhanging beam with a point load applied on its upper end via the stance stiffness coupling part (Fig. 4, g). The maximum deflection under load is located at this upper extremity and can be related to the applied point force F following beam theory [21]:

$$\delta_{max} = \frac{Fb^2 L}{3EI} \tag{1}$$

where b is the fulcrum to upper extremity distance, L is the beam length, $I = \frac{wh^3}{12}$ its inertia and E the Young modulus of the used material. These geometric quantities are depicted in Fig. 5 (right). Following the lever-arm principle, the maximum deflection and resulting joint torque τ_b can be written as a function of the knee angle θ and the arm length r_L (Fig. 5, left) separating the pulley main shaft and the upper end of the beam: $\delta_{max} = r_l \sin(\theta)$ and $\tau_b = 2Fr_L\cos(\theta)$. The factor 2 stands for the two symmetric beams. Combining these elements provides, with small angle approximation:

$$\tau_b = 2\left(\frac{3EIr_L^2}{b^2L}\right)\frac{\sin(2\theta)}{2} \approx \frac{6EIr_L^2}{b^2L}\,\theta \tag{2}$$

Therefore, the rotational stiffness is equal to $k_b = \frac{\tau_b}{\theta} = \frac{6EIr_L^2}{b^2L}$. The required beam Young modulus is obtained as:

$$E = \frac{b^2Lk_b}{6Ir_L^2} \tag{3}$$

The mechanism coupling and engaging this high stiffness spring works following a cam cleat principle, as depicted in Fig. 4. On each side of the prosthesis, two cams connect the pulley and transmission components. They are arranged in a double overarching configuration with the side appendage of the pulley (Figs. 3, g and 4, f). This appendage is located at a distance r_a from the pulley center (depicted in Fig. 4, step 6).

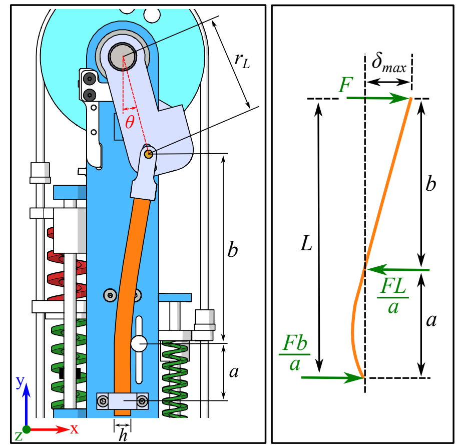

Fig. 5. Lateral view of the prosthesis in the middle of the weight acceptance phase (left) and diagram of the stance stiffness beam with simple support and overhang loading F (right). Representative dimensions and angles are: the distance between the fulcrum and the lower extremity of the beam a, the beam depth h, the knee flexion angle θ, the lever arm length r_L, the beam length $L = a + b$ and the beam maximum deflection δ_{max}.

In this mechanism, both rotating friction pawls ensure correct transmission of the spring torque relying on the principle of friction amplification. To this aim, the pawls are designed so that the friction between these and the coupling appendage pulls it further along, increasing the contact and thus the friction force. After engaging the appendage in-between the cams when coming to full extension at heel strike (Figs. 3 and 4, step 1), stance knee flexion can occur with the transmission of the spring resistive torque to the joint (Figs. 3 and 4, step 2). To prevent risks of falls due to incomplete knee extension at heel strike, the angular coverage of the pulley appendages is extended from 0 to 15°, providing robustness to the support function.

When the user returns to the full extension position at the end of the weight acceptance phase, two decoupling levers previously resting on a cam protrusion (Fig. 4, step 1) have pivoted and can disengage the system by keeping the cams in the open position (Fig. 4, step 3). This then allows the pulleys to flex again with no more coupling to the high-stiffness beams (Fig. 4, step 4). In order to prepare the next cycle, a reset system consisting of a cam (Fig. 3, h) and its spring-loaded follower (Fig. 3, b) fitted with two rods (Fig. 4, a+d) then allows moving both levers apart to allow the cams to return to their resting position (Fig. 4, step 5) after a triggering angular position is reached during swing.

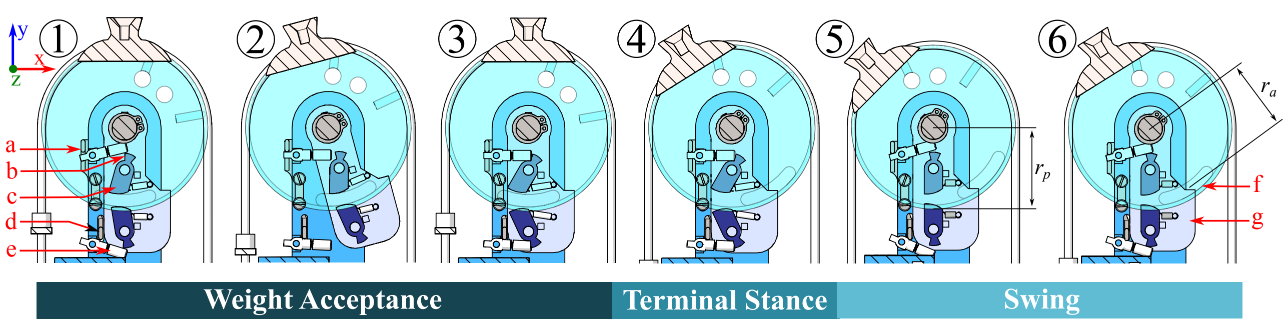

Fig. 4. Sectional detail view of the stance mechanism during an overground gait cycle. The observable components are: (a) upper lever reset mechanism, (b) cam protrusion, (c) coupling friction cam/pawl, (d) lower lever reset mechanism, (e) decoupling lever, (f) pulley side coupling appendage, and (g) stance stiffness beam to cam coupling.

This position is adjustable by changing the cam angular orientation on the main shaft. It has been set to 40° in the design presented in Fig. 3. At late swing, the coupling appendage returns to the cams, ready to catch them for the next cycle (Fig. 4, step 6).

B. Implementation of swing stiffness

The stiffness of the swing phase k_{sw} is implemented using two sub-systems. Using a cable-pulley transmission, both transform linear stiffness from spiral compression springs into joint rotational stiffness. Two cables (Fig. 3, i) transmit the efforts from various deformable elastic elements to render the different joint stiffnesses. This design choice allows working in translation rather than in rotation, and it is thus possible to exploit the volume of the calf to efficiently integrate the prosthesis mechanisms. In this way, rendering a rotational stiffness k_θ is achieved through a spring of linear stiffnesses k_l given by:

$$k_l = \frac{k_\theta}{r_p^2} \tag{4}$$

The swing mechanism is one of the two sub-systems and is used for implementing the negative part of the joint torque (flexion torque) from the swing stiffness curve. The positive torque (extension torque) of the swing stiffness curve is implemented via the double stiffness mechanism presented in Section III-C.

The swing mechanism implementation consists of two spiral compression springs (Fig. 3, n) acting on the carriage of a linear guide (Fig. 3, l), each accounting for half the swing stiffness ($k_{sw}/2$). When the knee joint flexion is below the rest position (ranging from full extension to 32° of flexion), a stopper (Fig. 3, j) coupled to both transmission cables contacts the carriage, enabling the transmission of spring forces to the joint pulleys through the connecting cable. This produces a torque flexing the knee joint with an unidirectional effect. Therefore, in order to obtain the extension torque part of the swing stiffness curve, a similar unidirectional effect is implemented in the double stiffness mechanism, as explained in the following subsection.

C. Double stiffness mechanism

The double stiffness mechanism is designed in order to render (i) the remaining part of the swing stiffness curve (positive torque) and (ii) the increased stiffness k_{sit} when reaching a defined angular position, allowing amplified sitting assistance through a larger torque decelerating body descent. Again, the system works by transforming the linear stiffness of compression springs into rotary joint stiffness via a cable-pulley transmission as governed by (4).

The operating principle of the stiffness variation mechanism is displayed in Fig. 6. Similarly to the swing mechanism, it is based on a linear guide whose carriage transmits its force to the joint via a cable stopper attached to the cable. However, in this case, springs in series are used to adapt the rendered stiffness. A first pair of springs (each of stiffness k_1) implementing the sitting stiffness k_{sit} (red solid line, Fig. 1) is in series with a single spring with lower stiffness k_2. These are represented in red and green respectively in Fig. 3 and 6. The equivalent stiffness k_{eq} of these springs is governed by the relationship:

$$k_{eq} = \begin{cases} \dfrac{2k_1k_2}{2k_1 + k_2} & \text{, if } \theta < 75^\circ \\ 2k_1 & \text{, else} \end{cases} \tag{5}$$

When the user starts sitting and flexes the knee from 0 to 75° (Fig. 6, steps 1-4), the equivalent stiffness is that of the series of both red springs ($2k_1 = k_{sit}$) with the green spring ($k_2 = 17$ Nm/rad). Due to the significant difference in these two values, the low-stiffness spring undergoes most deformations and the equivalent stiffness is the swing stiffness ($k_{eq} = 16$ Nm/rad, see Section II-C). Then, reaching 75°, the intermediate plate coupling the springs comes into contact with two stops blocking its linear motion (Fig. 6, step 4). From this point, the swing spring stiffness can no longer undergo deformations, such that only the pair of springs implementing sitting stiffness ($k_{eq} = 2k_1 = 220$ Nm/rad) remains. After 75°, the stiffer springs compress until seated (around 85°). Then, the knee extension locking mechanism (next subsection) is engaged such that the energy compressed in the swing and sitting springs is stored for future use. Note that this system offers intrinsic user adaptability since the stiffening position can be adjusted via the stopper screws.

D. Knee extension locking mechanism in seated position

The last mechanism allows to lock the extension torque supporting the stand-to-sit transition when fully seated. This

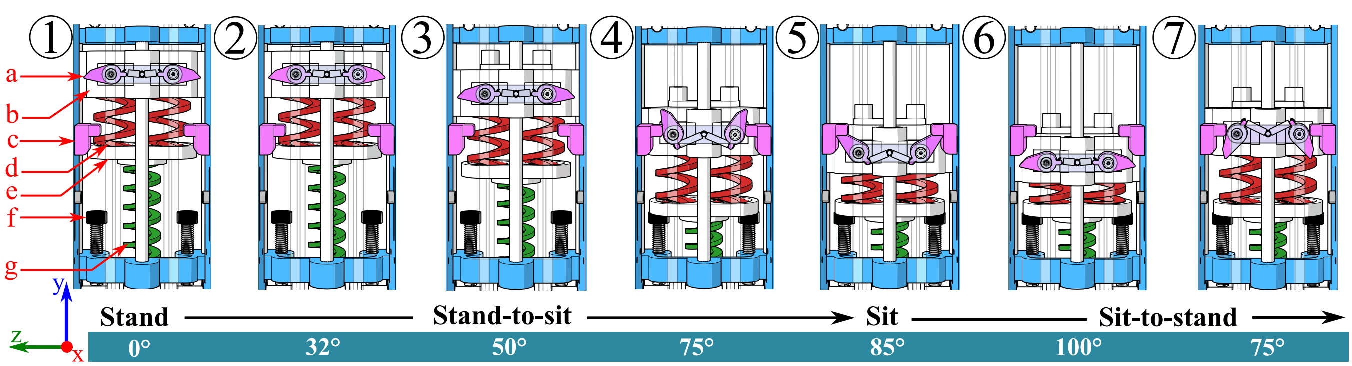

Fig. 6. Front view of the double stiffness and knee extension locking mechanisms during the stand-to-sit (steps 1-5) and sit-to-stand (steps 5-7) transitions. The main parts of the mechanisms are: (a) knee extension locking cam, (b) double stiffness carriage, (c) L-shaped locking support, (d) high stiffness sitting spring, (e) intermediate spring coupling plate, (f) adjustable linear motion stopper, and (g) swing spring (extension torque).

makes the rendered stiffness dropping to zero. This system is based on a cam assembly preventing the double stiffness mechanism carriage (Fig. 6, b) from moving backward after sitting.

When the cam system is inactive, it is maintained in a rest position via springs directly acting on the cams (Fig. 6, steps 1-3). As the knee flexes, the carriage of the double stiffness mechanism — to which are fixed the cams — moves down. At some angle (approx. 75°), the cams are forced into rotation when contacting a specific L-shaped support fixed to the main structure (Fig. 6, step 4). After progressing up to 85°, the cams are allowed to extend downwards but are limited by the body (vertical part) of the locking support. In this position, the leg (horizontal part) of the L-shaped support prevents the carriage from moving backward (Fig. 6, step 5), thus achieving the desired locking state.

To unlock the mechanism, we made a design choice requiring the user to further flex their knee while being in the seated position (approx. 100°), as shown in Fig. 6 (step 6). This makes both cams rotating downwards as passing the L-shaped body of the locking support. Once the cams have passed this position and are thus back in their resting position (spring loaded), the knee can go back to full extension as the cams can now move over the locking support (Fig. 6, step 7). This achieves extension torque unlocking in order to support sit-to-stand.

An important remark concerns the locked position (step 5). In this configuration, the cam action prevents the carriage from moving upwards. As the efforts are transmitted via a cable stop (Fig. 3, c) connecting both cables and pressing against the carriage when flexing the knee, this stop is free to separate from the carriage when it is locked. Therefore, when seated, the user can extend freely the prosthetic leg for convenience with virtually zero stiffness.

IV. Functional components dimensioning

In this section, the dimensioning of the functional elements of the main mechanisms is overviewed in order to assess the fabricability of the designed device.

A. Main pulley radius

The radius of the main pulleys r_p is a design choice affecting all the other mechanisms. In order to minimize the efforts in all sub-systems producing or transmitting the joint torque, r_p should be taken as large as possible, yet up to the point that it is not oversized with respect to a biological knee. Therefore, the external pulley radius r_p and the radius of its side coupling appendage r_a are fixed to 40mm and 35mm, respectively.

B. Spring stiffness and deflection

Springs are key elements of our device. In order to obtain the requirements in stiffness reported in Section II-C, compression springs are selected as they exhibit higher volumetric and mass energy densities than torsion or extension ones [4]. Following the choice to work in translation, the required linear stiffnesses can be obtained from the rotational ones using (4). This gives about 10 N/mm for the swing stiffness and 136 N/mm for the sitting stiffness. With the series spring stiffness Equation (5) the stiffnesses of the double stiffness mechanism are obtained: $k_1 = 136/2 = 68$ N/mm (two red springs in Fig. 6) and $k_2 = 11$ N/mm (single green spring in Fig. 6). The flexion stiffness of the swing mechanism implements the desired stiffness with a pair of parallel green springs (Fig. 3, n). The required linear deformations are 22.5 mm, 30 mm, and 17.4 mm for the swing flexion, swing extension, and sit springs, respectively. These springs can be found in the catalogs of typical mechanical element suppliers. It is worth noting that the springs implementing the different stiffnesses could be changed to adapt to multiple user weights. In addition, the range of motion and rest position can be adapted by changing the anchoring position of the cable stoppers.

Finally, the stance stiffness (290 Nm/rad) is obtained with both orange deformable beams (Fig. 3, k). Considering two beams of length $L = 128$ mm, with cross-sectional dimension $h = 5$ mm and $w = 12$ mm, the desired Young modulus of the beams should be equal to $E = 291$ GPa to obtain the desired stance stiffness with a position of the fulcrum $b = 93$ mm and a lever arm $r_L = 46$ mm. The position (b) of the fulcrum has been set to adapt for a 80kg user but this could be adapted to change the stiffness with the requirement of other users weight. The maximum beam deflection δ_{max} at its upper extremity is thus 12.7 mm. These characteristics can be found on the market for composite beams made of carbon fiber and epoxy resin.

C. Locking cams and support

The proper sizing of the cams and their supports is crucial to guarantee the effective functioning of the stance and seated knee extension locking mechanisms. Based on critical joint torques during weight acceptance (56 Nm) and sitting (67 Nm) for an 80kg individual and considering a safety factor $K_s = 1.5$, the tangential force on stance cams (4 cams) and normal force on sit cams (2 cams) can be derived as $F_{f,st} = 600$ N and $F_{N,sit} = 1260$ N. These forces are represented in Fig. 7. The contact forces on the supporting shafts can be derived based on the self-locking condition for the friction

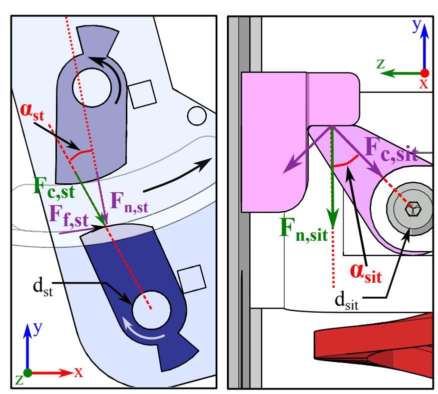

Fig. 7. Free-body diagram of the stance (left) and seated (right) cam locking mechanisms. The normal and friction forces (F_n and F_f) of the mechanisms lead to the derivation of the contact forces (F_c) depending on the contact angle α. This dictates the required supporting shaft diameter d.

cams relating the contact angle with the friction coefficient, i.e. $\alpha_{st} < \text{atan}(\mu)$. For a steel-to-steel contact ($\mu = 0.6$), this gives $\alpha_{st} < 31°$. Taking a safety margin to ensure proper self-locking, the contact angle for the stance mechanism is selected as $\alpha_{st} = 15°$. The contact angle for the sit mechanism is fixed to $\alpha_{sit} = 30°$. In this case, the system does not rely on friction to lock, the contact angle is selected based on geometric criteria to optimize available space. Therefore, contact forces are equal to $F_{c,st} = 2320$ N and $F_{c,sit} = 1090$ N. Supposing the worst case of two cantilever beams supporting the cams, with a length of $L_{st} = 5$ mm and $L_{sit} = 10$ mm for the stance and sit mechanism, respectively, and considering the bending stress equation from beam theory [21]:

$$\sigma_b = \frac{32M}{\pi d^3} < \sigma_y$$

where M is the bending moment resulting from the contact force on the shaft of diameter d. The minimum required beam diameters for a 1040 steel alloy ($\sigma_y = 413$ MPa) are $d_{st} = 5.3$ mm and $d_{sit} = 5.1$ mm for the stance and sit mechanisms respectively.

V. Conclusion and perspectives

This paper introduced a conceptual design incorporating three distinct stiffness levels, coupled with clutching and locking mechanisms, yielding to the embodiment of a completely passive knee prosthesis. This device should deliver assistance to an amputated user during both level ground walking and stand-to-sit plus sit-to-stand transitions. Therefore, the main innovation of the concept lies in its ability to adapt the knee joint stiffness in a purely passive manner relying on dedicated mechanisms to switch between the three stiffness levels. This results in the reproduction of the natural gait biomechanics as faithfully as possible. In addition, motion capabilities are enhanced with passive assistance while standing up and sitting down. Inspired by the knee angle-torque profile during these tasks, the study presented mechanisms for weight acceptance, swing assistance, and progressive stiffening during sitting. Importantly, all these mechanisms are adjustable to the user's weight and preferences. Dimensioning of these elements validates the device fabricability, presenting a promising outlook for the project. Potential enhancements for the device include dividing the swing stiffness into two parts for precise adjustment of stiffness during negative torque and achieving the desired angular position during late swing. Additionally, to accommodate various seat heights, making the locking angle of the seated position adjustable by moving the L lock position would be beneficial. Subsequent phases will involve validating the different sub-mechanisms on a dedicated test bench and assembling a prototype for tests with amputated users.

References

[1] W. Hughes, R. Goodall, J. D. Salciccioli, D. C. Marshall, A. H. Davies, and J. Shalhoub, "Editor's Choice - Trends in Lower Extremity Amputation Incidence in European Union 15+ Countries 1990-2017," *Eur. J. Vasc. Endovasc. Surg.*, vol. 60, no. 4, pp. 602–612, Oct. 2020. DOI:10/gg69h5

[2] N. Walter, V. Alt, and M. Rupp, "Lower Limb Amputation Rates in Germany," *Medicina (Kaunas)*, vol. 58, no. 1, p. 101, Jan. 2022. DOI:10/gtbrb4

[3] K. Khalil, "Healthcare Summit on War Zone Medicine scheduled for Kyiv," Nov. 2023. https://www.medicaldevice-network.com/news/healthcare-summit-on-war-zone-medicine-scheduled-for-kyiv/

[4] E. J. Rouse, L. M. Mooney, and H. M. Herr, "Clutchable series-elastic actuator: Implications for prosthetic knee design," *Int. J. Robot. Res.*, vol. 33, no. 13, pp. 1611–1625, Nov. 2014. DOI:10/f6nbs2

[5] L. Flynn, J. Geeroms, R. Jimenez-Fabian, S. Heins, B. Vanderborght, M. Munih, R. Molino Lova, N. Vitiello, and D. Lefeber, "The Challenges and Achievements of Experimental Implementation of an Active Transfemoral Prosthesis Based on Biological Quasi-Stiffness: The CYBERLEGs Beta-Prosthesis," *Front. Neurorobot.*, vol. 12, 2018. DOI:10/gfrpqk

[6] M. Tran, L. Gabert, S. Hood, and T. Lenzi, "A lightweight robotic leg prosthesis replicating the biomechanics of the knee, ankle, and toe joint," *Sci. Robot.*, vol. 7, no. 72, p. 3996, Nov. 2022. DOI:10/gq956h

[7] https://www.ossur.com/en-us/prosthetics/knees/power-knee

[8] https://www.rbionics.com/products/prosthetic-knee/

[9] S. C. Culver, L. G. Vailati, D. C. Morgenroth, and M. Goldfarb, "A new approach to a powered knee prosthesis: Layering powered assistance onto strictly passive prosthesis behavior," *Wearable Technol.*, vol. 4, p. e21, Jan. 2023. DOI:10/gtb9df

[10] S. Heins, L. Flynn, H. Laloyaux, J. Geeroms, D. Lefeber, and R. Ronsse, "Compliant Control of a Transfemoral Prosthesis by combining Feed-Forward and Feedback," in *2020 8th IEEE RAS/EMBS Int. Conf. Biomed. Robot. Biomechatron.*, Nov. 2020, pp. 452–458.

[11] W. Liang, Z. Qian, W. Chen, H. Song, Y. Cao, G. Wei, L. Ren, K. Wang, and L. Ren, "Mechanisms and component design of prosthetic knees: A review from a biomechanical function perspective," *Front. Bioeng. Biotechnol.*, vol. 10, 2022. DOI:10/gtb9dp

[12] M. Murabayashi and K. Inoue, "New function and passive mechanism of transfemoral prosthetic knee for running safely," in *2022 44th Annu. Int. Conf. IEEE Eng. Med. & Biol. Soc.*, July 2022, pp. 4334–4337. https://ieeexplore.ieee.org/document/9870830

[13] T. Ramakrishnan, M. Schlafly, and K. Reed, "Biomimetic Transfemoral Knee with a Gear Mesh Locking Mechanism," *Int. J. Eng. Res. Innov.*, vol. 8, no. 2, pp. 30–38, Jan. 2016.

[14] V. N. M. Arelekatti and A. G. Winter, "Design of a fully passive prosthetic knee mechanism for transfemoral amputees in India," in *2015 IEEE Int. Conf. Rehabilit. Robot.*, Aug. 2015, pp. 350–356, iSSN: 1945-7901. https://ieeexplore.ieee.org/document/7281224

[15] K. Shamaei, P. C. Napolitano, and A. M. Dollar, "Design and Functional Evaluation of a Quasi-Passive Compliant Stance Control Knee–Ankle–Foot Orthosis," *IEEE Transactions Neural Syst. Rehabilit. Eng.*, vol. 22, no. 2, pp. 258–268, Mar. 2014. DOI:10/gtb9dk

[16] H. L. Bartlett, S. T. King, M. Goldfarb, and B. E. Lawson, "Design and Assist-As-Needed Control of a Lightly Powered Prosthetic Knee," *IEEE Transactions Med. Robot. Bionics*, vol. 4, no. 2, pp. 490–501, May 2022. DOI:10/gtb9dj

[17] S. C. Culver, L. G. Vailati, and M. Goldfarb, "A Power-Capable Knee Prosthesis With Ballistic Swing-Phase," *IEEE Transactions Med. Robot. Bionics*, vol. 4, no. 4, pp. 1034–1045, Nov. 2022. DOI:10/gq9q8m

[18] T. Kikuchi, R. Fujino, K. Igarashi, and K. Koganezawa, "Non-Energized Above Knee Prosthesis for Stairs Walking with Synergetic Interaction Between Knee and Ankle Joints," in *2018 IEEE Int. Conf. Robot. Biomim.*, Dec. 2018, pp. 674–679. https://ieeexplore.ieee.org/document/8665171

[19] R. Unal, S. Behrens, R. Carloni, E. Hekman, S. Stramigioli, and B. Koopman, "Conceptual Design of a Fully Passive Transfemoral Prosthesis to Facilitate Energy-Efficient Gait," *IEEE Transactions Neural Syst. Rehabilit. Eng.*, vol. 26, no. 12, pp. 2360–2366, Dec. 2018. DOI:10/gtb9dh

[20] L. Zhang, G. Liu, B. Han, Z. Wang, Y. Yan, J. Ma, and P. Wei, "Knee Joint Biomechanics in Physiological Conditions and How Pathologies Can Affect It: A Systematic Review," *Appl. Bionics Biomech.*, vol. 2020, p. 7451683, Apr. 2020. DOI:10.1155/2020/7451683

[21] R. C. Juvinall and K. M. Marshek, *Fundamentals of Machine Component Design*, seventh edition ed. Wiley, June 2021.